

## Article

# Relationship of Ecosystem Services in the Beijing–Tianjin–Hebei Region Based on the Production Possibility Frontier

Jinjin Wu <sup>1</sup>, Xueru Jin <sup>2</sup>, Zhe Feng <sup>1,3,\*</sup> , Tianqian Chen <sup>4,5</sup>, Chenxu Wang <sup>4,5</sup>, Dingrao Feng <sup>1</sup> and Jiaqi Lv <sup>1</sup>

<sup>1</sup> School of Land Science and Technology, China University of Geosciences, Beijing 100083, China; jinjinwu@cugb.edu.cn (J.W.); fengdingrao@cugb.edu.cn (D.F.); JiaqiLv@cugb.edu.cn (J.L.)

<sup>2</sup> School of Urban Planning and Design, Peking University, Shenzhen 518055, China; jinxueru@stu.pku.edu.cn

<sup>3</sup> Technology Innovation Center of Land Engineering, MNR, Beijing 100035, China

<sup>4</sup> Faculty of Geographical Science, School of Natural Resources, Beijing Normal University, Beijing 100857, China; tianqianchen@cugb.edu.cn (T.C.); 1012172119@cugb.edu.cn (C.W.)

<sup>5</sup> State Key Laboratory of Earth Surface Processes and Resource Ecology, Faculty of Geographical Science, Beijing Normal University, Beijing 100875, China

\* Correspondence: zhefeng@cugb.edu.cn

**Abstract:** The supply and demand of ecosystem services are affected by land use. Only a few studies have conducted in-depth quantitative analyses. This study adopted the Beijing–Tianjin–Hebei region as the research area. The CLUMondo model was adopted to infer the land-use pattern under protection, development, and natural scenarios in 2035. Moreover, the InVEST model was utilized to evaluate carbon sequestration, water yield, and soil conservation under multiple land-use patterns. The production possibility frontier was drawn to visualize the trade-off relationship further. The trade-off intensity index was calculated to quantify the magnitude of the trade-off. (1) Under the development scenario, the accelerated expansion of urbanized land will occupy a large amount of arable and forest land, which should be planned and controlled. (2) The trade-off and synergistic relationships could be transformed under the different land-use scenarios. (3) The production possibility frontier curve for each ecosystem service trade-off and the optimal value of the trade-off configuration were plotted for the different scenarios. The trade-off intensity of ecosystem services was also calculated. This study combined ecosystem services with land-use regulations and revealed the link between ecosystem services and regional land-use pattern change. The aim is to provide a reference for the synergistic progress of the ecological economy in the Beijing–Tianjin–Hebei region.

**Keywords:** ecosystem services; trade-offs; production possibility frontier; scenario simulation; land-use change



**Citation:** Wu, J.; Jin, X.; Feng, Z.; Chen, T.; Wang, C.; Feng, D.; Lv, J. Relationship of Ecosystem Services in the Beijing–Tianjin–Hebei Region Based on the Production Possibility Frontier. *Land* **2021**, *10*, 881. <https://doi.org/10.3390/land10080881>

Academic Editor: Richard C. Smardon

Received: 21 July 2021

Accepted: 20 August 2021

Published: 22 August 2021

**Publisher's Note:** MDPI stays neutral with regard to jurisdictional claims in published maps and institutional affiliations.



**Copyright:** © 2021 by the authors. Licensee MDPI, Basel, Switzerland. This article is an open access article distributed under the terms and conditions of the Creative Commons Attribution (CC BY) license (<https://creativecommons.org/licenses/by/4.0/>).

## 1. Introduction

Ecosystems provide natural environmental conditions and functions that sustain human survival. The benefits that humans obtain directly or indirectly from ecosystems are called ecosystem services [1], which are essential to maintaining the well-being of humans. The concept of ecosystem service was established to improve and protect the ecological environment [2]. Several scholars have conducted extensive research on ecosystem services [3,4]. The Millennium Ecosystem Assessment clarified the contribution of ecosystem services to human well-being. Ecosystem services refer to the full benefits that humans gain from natural ecosystems [5]. Considering the relationship between ecosystem services and ecosystem structure, process and function, ecosystem services usually include four categories: provisioning, regulating, cultural, and supporting services [6,7]. Approximately 60% of ecosystem degradation in the past 50 years was due to the urbanization and population growth worldwide. Therefore, research on ecosystem services has become increasingly urgent. Ecosystems and ecosystem services are widely studied

worldwide [8]. These studies mainly include ecosystem service assessment, ecosystem service trade-off analysis [1,9–11], and investigation of land management policies based on ecosystem services [12].

Ecosystem services show trade-off and mutual-gain relationships. Trade-off refers to the situation in which an increase in certain types of ecosystem services decreases other types of ecosystem services. A trade-off often occurs between supporting and regulating services [13]. Synergy refers to the situation wherein the change trends of two or more ecosystem services are the same [14]. Irrelevant means that no evident connection exists between various ecosystem services [15]. The commonly used research methods for trade-offs and synergies include statistical, spatial analysis, ecosystem service mobility analysis, and scenario simulation [16]. Correlation analysis is mainly used in statistical methods to analyze changes in ecosystem services in quantitative terms. It is generally based on the correlation coefficient between ecosystem services and used to determine whether a link exists between services. The degree and direction of correlation are determined by the magnitude of the absolute value of the correlation and the direction of positive and negative correlations [17]. Meanwhile, the spatial analysis method mainly uses geographic information system technology to compare the spatial patterns and scale effects of ecosystem services. It is conducive to the analysis of the mechanism of trade-offs between ecosystem service. The analysis method of ecosystem service liquidity is mainly based on the principle of network analysis technology, and the scenario simulation method mainly uses models to simulate different land-use patterns. The most widely used among these models is the comprehensive evaluation and trade-off model of ecosystem services based on scenario simulation (InVEST model), which was jointly developed by Stanford University, The Nature Conservancy, and the World Wide Fund for Nature. The purpose of the model is to simulate changes in the ecosystem service quality and ecosystem service value under simulated land-use/cover scenarios. The data required by the model are concise. In addition, the resulting exported data are rich in content. Hence, the method can quantitatively analyze abstract ecosystem services [18].

Many scholars at home and abroad have conducted research on the balance of ecosystem services. In research fields, trade-offs or synergies are common among various ecosystem services [19]. Even in the same region, trade-offs and synergies change during different periods. For example, Wei et al. found that carbon storage and material production in the Yellow River Delta changed from being a synergistic effect to being a trade-off effect in 2008 [20]. Differences were also observed in the relationship between ecosystem services in different regions [21]. Li et al. reported that the synergistic relationship among food production, water yield, and soil conservation in Nansi Lake Basin mainly occurs in and around the Guanzhong Basin. The trade-off relationship is primarily manifested in the southwestern part of Guanzhong Basin (e.g., woodlands as well as pastures) and inland areas [22].

The production possibility frontier (PPF) is an economic concept that is typically used to express visually the different quantity combinations of two commodities effectively produced by the economy (or subject) under limited production resources [23]. A point on the curve represents the price between two commodities in a trade-off relationship. The price measures each additional unit of one commodity in the cost and how much the other commodity loses [24]. This curve shows that as resources are transferred from the other commodity, increasing the output of one commodity reduces the maximum output of another commodity [25]. It can also illustrate the trade-offs between ecosystem services and visualize their optimal combination in the trade-off relationship [26,27]. Stosch et al. used the PPF curve to quantify stakeholders' assessment of the shape and uncertainty of PPF in the trade-off between crop production and ecological environment of the freshwater system [28]. Zavalloni et al. evaluated the role of spatial information in the trade-off between aquaculture and nursery habitat functions. By using a bio-economic model to map the PPF of mangroves, the model visualizes the most beneficial combination of wild shrimp and farmed shrimp [23]. To describe the trade-offs between ecosystem services

quantitatively, Li et al. utilized Bayesian belief networks to analyze the efficiency of ecosystem services [29]. In line with the distribution of the three ecosystem services in different scenarios, a three-dimensional coordinate system was drawn [30], and the optimized target efficiency curve was obtained.

Land-use change is an important factor that affects trade-offs in ecosystem services [31,32]. Given population growth and urbanization acceleration, the overall land-use pattern is constantly changing, thus affecting the balance of ecosystem services [26,33]. Scenario simulation can be used to select a series of socio-economic and ecological indicators that can be combined with relevant policy planning to find out how human activities and land-use pattern changes influence the balance of ecosystem services [34]. Existing studies have evaluated the relationship among multiple ecosystem services by simulating various land-use scenarios [30,35,36]. Therefore, ecosystem service evaluation under the simulated land-use change scenarios is an effective method to study environmental protection policies. This approach contributes a new idea for identifying the relationship between ecosystem services [37]. It simulates land-use change scenarios on a small scale and fully considers the impact of land-use intensity during the simulation [38]. The final result can reflect the current intensity of human activities and the impact of social and economic development on land-use patterns [39]. The model has been widely used in land-use simulation [40,41].

The introduction of the production possibility boundary provides a new idea for the quantification of the trade-off relationship. On the basis of this method, the strength of the trade-off between different combinations can be quantitatively described, and the trade-off between different services can be displayed directly. A few studies on the trade-off relationship between ecosystem services have used this method.

The Beijing–Tianjin–Hebei region is a highly dense political, economic, cultural, and populated area comprising northern cities in the country. It occupies a place in the country's overall development strategy and economic structure. In 2014, the Chinese government proposed the Beijing–Tianjin–Hebei Coordinated Development Strategy, which organically integrates the advantageous resources of the three places. This integration has increased the diversity of cross-regional cooperation. The region shares the same development goals in ecology, economy, and society. By evaluating ecosystem services in the Beijing–Tianjin–Hebei region under different land-use scenarios, this study analyzes the correlation and trade-off between different services. The PPF curve is adopted to demonstrate the strength of the trade-off between these services visually. Such a depiction provides a reference foundation for the new pattern of coordinated progress in the region.

## 2. Data and Methods

### 2.1. Study Area

The Beijing–Tianjin–Hebei region is the capital economic circle in China, covering Beijing, Tianjin, and Hebei provinces. It has a large area and gradually tilts from the northwest to the southeast. The annual average temperature is approximately 11 °C and the annual average precipitation is approximately 500 mm. The regional land-use types present a significant decrease in arable land and a large increase in urban and rural built-up land. Given the acceleration of urbanization, the land-use pattern in this area has gradually become increasingly complicated.

The study area occupies approximately 218,000 km<sup>2</sup>, with the population more than 100 million. Given the acceleration of urbanization, rapid population growth, and backward ecological infrastructure in recent years, the consumption of regional natural resources has become particularly high, and a series of ecological and environmental issues, such as air pollution, land desertification, and soil erosion, have become increasingly prominent. The region is faced with the status quo of excessive ecological load [42], which restricts further regional development and progress. Land-use and cover changes depend largely on nature, social economy, and human activities. The location of the study area is shown in Figure 1.

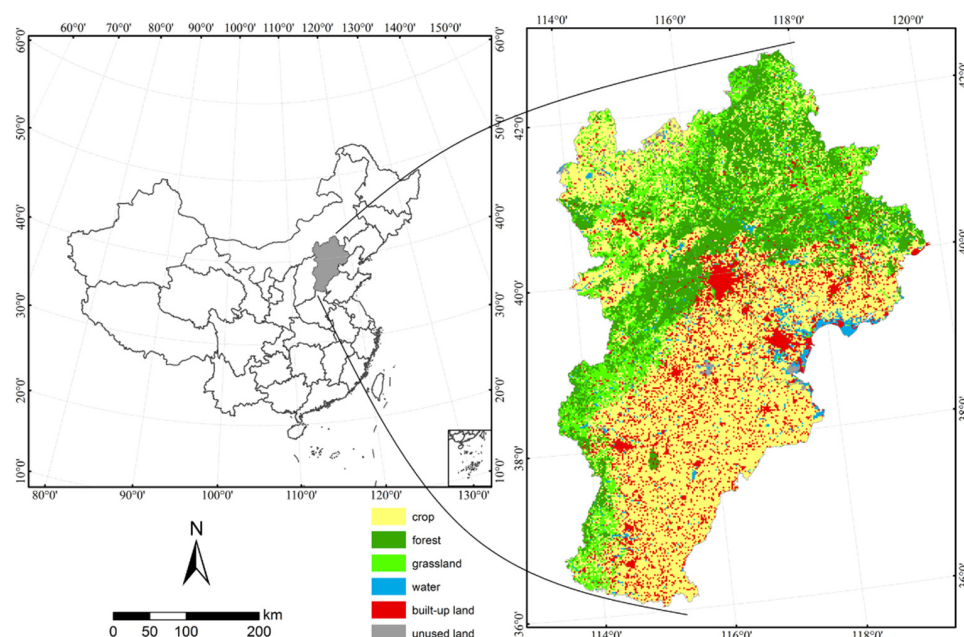


**Figure 1.** Location of the study area in 2015.

## 2.2. Data Sources

The data are shown in Table 1. Land-use data have been separated into six types: arable land, woodland, grassland, water, urbanized land, and unused land. Infrastructure elements were obtained by importing land-use data into ArcGIS for processing. Data preprocessing and extraction were performed in the ArcGIS 10.2 platform. The spatial resolution of raster data was  $1 \text{ km} \times 1 \text{ km}$ , and Krasovsky\_1940\_Albers projection was used.

**Table 1.** Data information table.

Data Name	Spatial Resolution	Source	Website
Administrative boundaries	/	Resource and Environment Data Cloud Platform	<a href="http://www.resdc.cn/">http://www.resdc.cn/</a> (accessed on 5 April 2021)
Land-use type	1 km	Resource and Environment Data Cloud Platform	<a href="http://www.resdc.cn/">http://www.resdc.cn/</a> (accessed on 5 April 2021)
Digital elevation model (DEM)	90 m	Geospatial Data Cloud site	<a href="http://www.gscloud.cn/">http://www.gscloud.cn/</a> (accessed on 5 April 2021)
GDP	1 km	National Bureau of Statistics of the People's Republic of China	<a href="http://www.stats.gov.cn">http://www.stats.gov.cn</a> (accessed on 5 April 2021)
Traffic network elements	/	Openstreetmap	<a href="https://www.openstreetmap.org/">https://www.openstreetmap.org/</a> (accessed on 5 April 2021)
Infrastructure elements	/	Extracted from Land-Use Classification Map	<a href="http://www.resdc.cn/">http://www.resdc.cn/</a> (accessed on 5 April 2021)
Grain output	/	National Bureau of Statistics of the People's Republic of China	<a href="http://www.stats.gov.cn/">http://www.stats.gov.cn/</a> (accessed on 16 April 2021)
Soil sandy loam clay content	1 km	Resource and Environment Data Cloud Platform	<a href="http://www.resdc.cn/">http://www.resdc.cn/</a> (accessed on 16 April 2021)
Soil depth	1 km	Cold and Arid Regions Sciences Data Center	<a href="http://westdc.westgis.ac.cn/data/">http://westdc.westgis.ac.cn/data/</a> (accessed on 16 April 2021)
Plant available water content	1 km	Cold and Arid Regions Sciences Data Center	<a href="http://westdc.westgis.ac.cn/data/">http://westdc.westgis.ac.cn/data/</a> (accessed on 16 April 2021)
Evapotranspiration (ET0)	1 km	CGIAR Consortium for Spatial Information	<a href="https://cgiarcsi.community/">https://cgiarcsi.community/</a> (accessed on 16 April 2021)
Vegetation index (NDVI)	1 km	NASA's Earth Observing System Data and Information System	<a href="https://search.earthdata.nasa.gov/">https://search.earthdata.nasa.gov/</a> (accessed on 16 April 2021)
Precipitation	0.1°	Goddard Earth Sciences Data and Information Services Center	<a href="https://disc.gsfc.nasa.gov/">https://disc.gsfc.nasa.gov/</a> (accessed on 16 April 2021)
Temperature	1 km	Resource and Environment Data Cloud Platform	<a href="http://www.resdc.cn/">http://www.resdc.cn/</a> (accessed on 16 April 2021)
Population density	1 km	Resource and Environment Data Cloud Platform	<a href="http://www.resdc.cn/">http://www.resdc.cn/</a> (accessed on 5 April 2021)

### 2.3. Method

#### 2.3.1. Scenario Simulation

Ecosystem supply and ecosystem relationships are deeply affected by land-use changes [43]. The CLUMondo model is a new method for design of land-use change patterns; it is driven by the regional commodity demand and considers the factors of the conversion between different regions to simulate changes in the land system [38]. By using the CLUMondo model and with 2015 as the initial year, different driving factors were set, and the conversion parameters between different land-use types were continuously revised according to demand. The land-use conditions of the study area in 2035 under the three scenarios were simulated [44]. This research analyzed and explained land-use problems in the study area through land-use change. It established relevant models to understand the process of land-use change and the driving force for this change. The study also simulated and predicted future scenarios to determine the trend of future land-use changes accurately [45]. Initially, this research analyzed the land-use changes in 2005–2015 and referred to the research results of other scholars [46,47]. Ten natural, socio-economic, and demographic factors were recognized as driving factors. The information on the driving factors is shown in Table 2. The selection of drivers is a key factor in the spatial pattern of land-use types. The area under the receiver operating curve (AUC) is an assessment index to measure the calculation accuracy of a regression model. The results of this study suggested that the AUC values between each category and the driving factors were all over 0.75. Hence, the selected of driving factors can comprehensively explain the spatial patterns of land-use types. The use of forest and built-up land area was adopted as the demand factor. The CLUMondo model was utilized to simulate and predict land-use changes under various scenarios for exploring the trade-off relationship between multiple ecosystem services in each scenario.

**Table 2.** Driver list.

First Class	Second Class	Third Class
Natural factors	Terrain	Elevation Slope
	Climate	Annual precipitation Distance from National Highway Distance from Provincial Highway
Socio-economic factors	Road	Distance from Railway Distance from county/district center
	Economy	Grain production Total regional output value
Population factors	Population	Population density

The first scenario is the natural scenario, which is consistent with the analysis of land-use change in 2005–2015. Land-use change is expected to continue according to the existing natural development pattern until 2035; hence, no special constraints were set for the CLUMondo model.

The next scenario is the development scenario, which accelerates the urbanization process based on the overall land-use planning and socio-economic development in the Beijing–Tianjin–Hebei region. It converts a large amount of arable, forest, and unused land into built-up land. In this scenario, the conversion resistance value for all land-use types was set to 1.

In the conservation scenario, the ecological environmental in the Beijing–Tianjin–Hebei region is vigorously protected. The area of arable, forest, and grassland that is converted to built-up land is strictly limited. In addition, the development of urbanization is slowed down. In this scenario, the conversion resistance of arable, forest, and grassland to built-up land was zero.

### 2.3.2. Water Yield

In this work, the annual water yield module of the InVEST model was used to assess the annual water yield of the Beijing–Tianjin–Hebei region in 2035 under multiple scenarios. The water content module combines the land-use type, soil depth, topography, climate, and other reasons based on the Budyko hydrothermal coupling balance hypothesis and the annual average precipitation [48]. The formula precipitation minus the actual evaporation was used to calculate the grid water content.

$$Y_{xj} = \left(1 - \frac{AET_{xj}}{P_x}\right) P_x, \quad (1)$$

where  $Y_{xj}$  is the annual water yield of grid unit  $x$  on land cover type  $j$ . It mainly includes surface runoff, soil water content, litter water holding capacity, and canopy interception.  $AET_x$  is the annual actual evapotranspiration of pixel  $x$ , and  $P_x$  is the annual precipitation of pixel  $x$ .

The  $Z$  value, which is a seasonal constant characterizing rainfall characteristics, must be inputted to the water yield model. This study refers to scholars' research on precipitation characteristics and set the  $Z$  value to 3.8 [43]. The biophysical properties of each land-use type involved in the model are illustrated in Table 3.

**Table 3.** Biophysical properties of each land-use type.

Land-use Type	Arable Land	Woodland	Grassland	Water	Built-Up Land	Unused Land
Root_depth (mm)	300	5000	500	1	1	1
Kc	0.3	0.85	0.65	1	0.23	0.1

### 2.3.3. Soil Conservation

Soil conservation is an important ecosystem service for the Beijing–Tianjin–Hebei region. The sediment delivery ratio module of the InVEST model was used in this research to evaluate the soil conservation under different scenarios in 2035. Given that the SDR module is based on the universal soil loss equation (USLE), which considers the capability of the site itself to intercept upstream sediment and adds sediment retention to the reservoir data, the results of the model are highly realistic and scientifically accurate. Soil conservation, potential soil loss, and actual soil loss are calculated as follows [48]:

$$SC_i = RKLS_i - USLE_i, \quad (2)$$

$$RKLS_i = R_i \cdot K_i \cdot LS_i, \quad (3)$$

$$USLE_i = R_i \cdot K_i \cdot LS_i \cdot C_i \cdot P_i, \quad (4)$$

where  $USLE$  is the actual soil loss in the original land-use cover,  $RKLS$  is the potential soil loss for bare soil,  $R$  is the rainfall erosivity factor,  $K$  is the soil erodibility factor,  $LS$  is the slope length–gradient factor,  $C$  is the crop–management factor, and  $P$  is the support practice factor.

The values of  $C$  and  $P$  combined with the characteristics of the study area and information previous studies are shown in Table 4 [49].

**Table 4.** The value of  $C$  and  $P$  of each land-use type.

Land-Use Type	Arable Land	Woodland	Grassland	Water	Built-Up Land	Unused Land
$C$	0.25	0.63	0.19	0	0	1
$P$	0.45	0.6	0.4	0	0	1

### 2.3.4. Carbon Storage

The carbon storage and sequestration model was used to select distribution of surface land-use and cover types for the calculation and analysis of the four basic carbon pools. Then, the module was utilized to generate a spatial distribution map of carbon storage. In this work, the aboveground biogenic carbon stock and the below-ground biogenic carbon stock were combined into vegetation carbon stock, which was not considered in this study because dead organic carbon stock is difficult to observe, and its stock is unavailable. The carbon storage calculation principle is as follows [48]:

$$C_{tot} = C_{above} + C_{below} + C_{soil} + C_{dead} \quad (5)$$

where  $C_{tot}$  is the total regional carbon storage,  $C_{above}$  is the aboveground biological carbon storage,  $C_{below}$  is the underground biological carbon storage,  $C_{soil}$  is the soil carbon storage, and  $C_{dead}$  is the dead organic carbon storage.

With reference to previous studies [50], the carbon density adopted in this research refers to the calculation of the carbon density of each carbon pool in the Beijing–Tianjin–Hebei region, as shown in Table 5.

**Table 5.** The carbon density for each land-use type (Mg/ha).

Land-Use Type	C_Above	C_Below	C_Soil	C_Dead
Arable land	3.38	47.83	103.01	9.82
Woodland	25.13	68.69	225.11	14.11
Grassland	20.92	51.27	94.93	10.55
Water	0	0	0	0
Built-up land	0	0	74.12	0
Unused land	0	0	0	0

### 2.4. Plotting the PPF Curve

In this work, the trade-off among the water yield, soil conservation, and carbon storage was expressed as PPF. First, the values of each ecosystem service were extracted, and the trade-offs and synergies between two ecosystem services were analyzed using the correlation analysis tool in R language. Second, the two ecosystem services presenting trade-offs were normalized to values between 0 and 1 after processing. Lastly, the normalized layers of the two ecosystem services were divided to obtain the ratio layer. Each cell in the ratio layer represented the ratio of the two ecosystem services in the corresponding geographic location. Then, each cell in the ratio layer was arranged in ascending order, and the values of the two ecosystem services in the corresponding geographic location were summed up. The curves were drawn based on the final results. The best trade-off values of the two ecosystem services were visualized [26,51].

The outcome of the changes in the research setting trade-offs reveals the best combination of the two ecosystem services [20]. On this basis and with reference to previous studies, the shortest distance from the mean point to the curve corresponding to the two services is represented as the trade-off intensity. Assuming that the coordinates of the mean point are at the  $(x_0, y_0)$  position and the equation of the curve is  $g = f(x)$ , the coordinates of any point on the curve are  $(x, g)$ . The distance calculation formula is as follows:

$$H = |(x_0, y_0) - (x, g)| = \sqrt{[x_0 - x]^2 + [y_0 - g]^2}. \quad (6)$$

Therefore, the strength of the trade-off is  $H_{min}$ . A large value of  $H_{min}$  indicates a strong trade-off relationship. A small value of  $H_{min}$  indicates a weak trade-off relationship.

### 3. Results and Analysis

#### 3.1. Analysis of Land-Use Simulation Results under Different Scenarios

Under the conservation scenario, in 2035, the area of arable land will decrease by 0.76%, the area of woodland will increase by 12.22%, the area of built-up land will increase by 28.72%, the water area will decrease by 10.91%, and the area of unused land will decrease by 8.13%. Under the development scenario, the rate of urbanization will accelerate sharply in 2035. The area of arable land will decrease by 15.22%, the area of woodland will decrease by 5.94%, the area of built-up land will increase by 95.65%, the water area will decrease by 28.89%, and the area of unused land will decrease by 12.98%. Compared with the situation in 2015, the area of each category shows evident changes. Under the natural scenario, in 2035, the area of arable land will decrease by 2.72%, the area of woodland will decrease by 2.31%, the area of built-up land will increase by 45.96%, the water area will decrease by 8.63%, and the area of unused land will decrease by 7.96%.

Comparison of the three scenarios showed that the increase and decrease in each category in the natural scenario were in the middle. The area of built-up land in the development scenario increased the most, and only the area of woodland in the conservation scenario showed an increasing trend. The kappa values of all land-use types were above 0.8, indicating that the simulation results are highly consistent with the actual land-use and that the accuracy of the model can meet the simulation requirements (Figure 2).

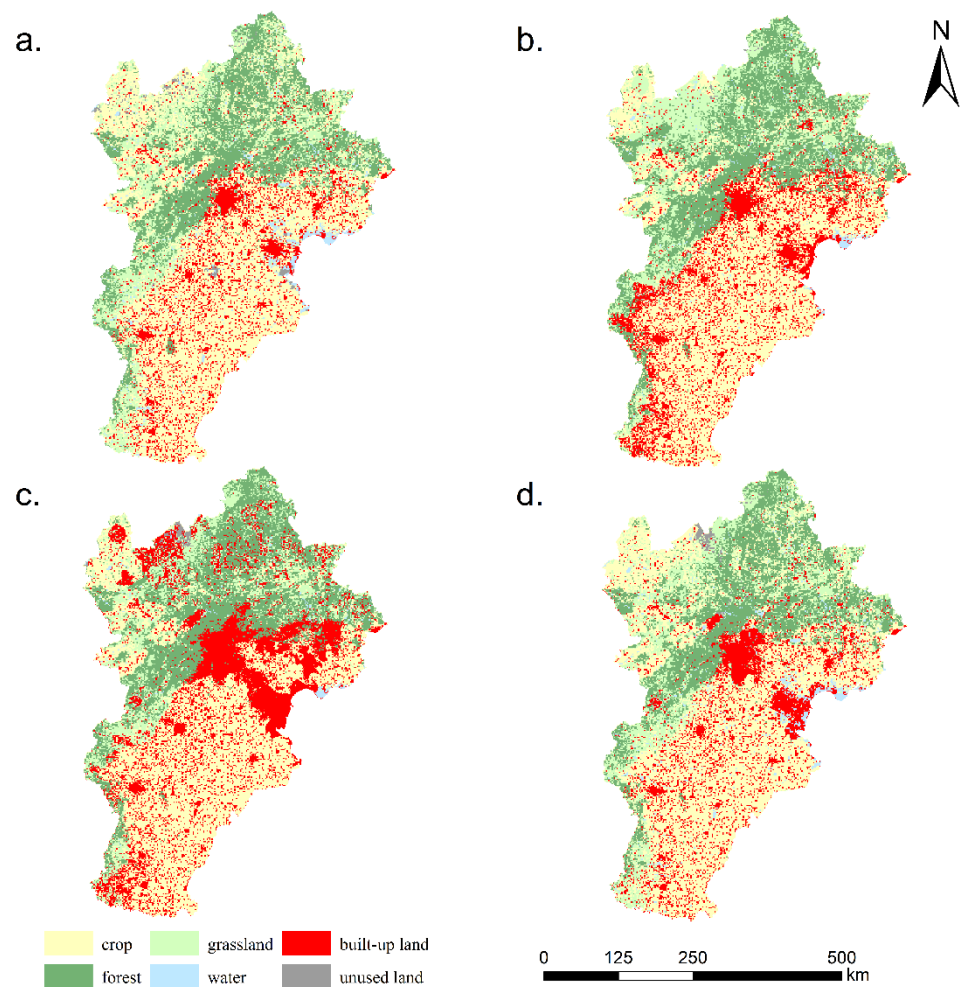


**Figure 2.** Land-use scenario simulation results. (a) 2015; (b) conservation scenario; (c) development scenario; (d) natural scenario.



### 3.2. Spatial Distribution of Ecosystem Services

The distributions of water yield under each scenario change are shown in Figure 3. Compared with the maximum value of 415.6 mm in 2015, the maximum value of water yield under the conservation and development scenarios increased and reached 574.8 and 596.1 mm, respectively, whereas the value for the natural scenario remained essentially unchanged. Under the conservation scenario, the water yield in the Beijing–Tianjin–Hebei region increased compared with the level in 2015; the high values were mainly in the arable areas in the east, and the low values were mainly in the mountainous forest areas in the northwest. The pattern of water yield capacity in the Beijing–Tianjin–Hebei region changed significantly, showing a significant increase in water yield capacity in the forest–grassland area in the north and a decrease in water yield capacity around Beijing and Tianjin because of the expansion of urbanized land under the development scenario. The natural scenario showed little change in water yield capacity in the Beijing–Tianjin–Hebei region.

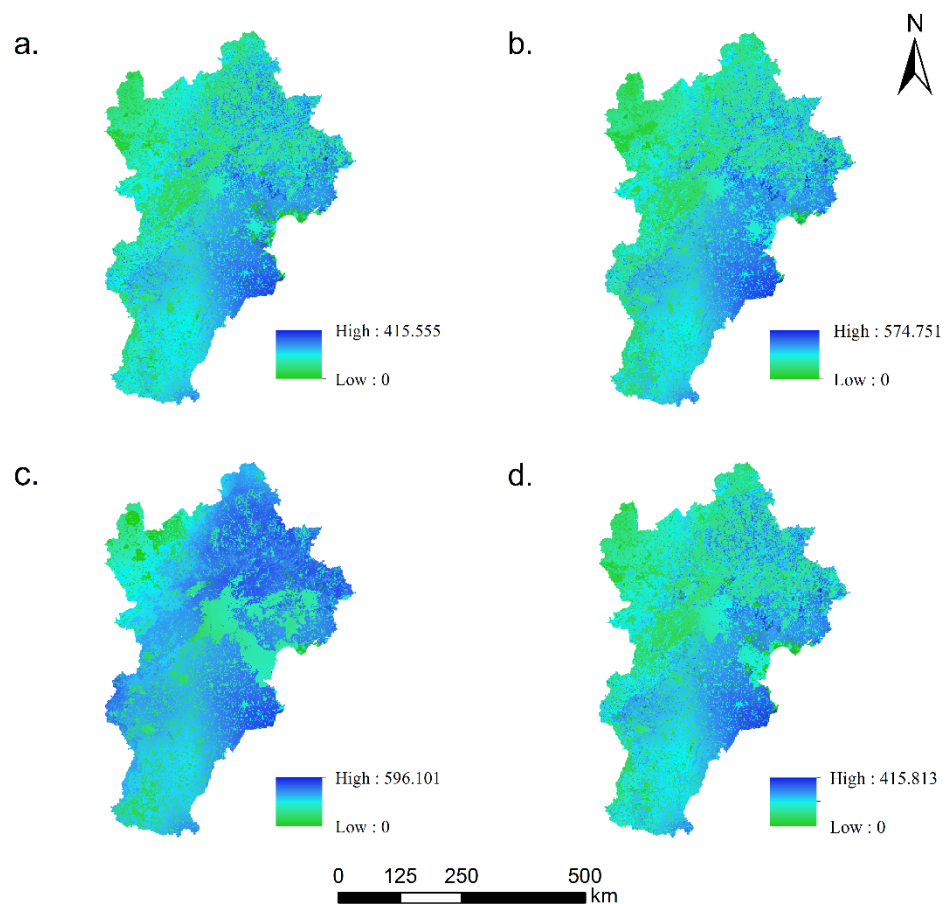


**Figure 3.** Distribution of water yield under different scenarios. (a) 2015; (b) conservation scenario; (c) development scenario; (d) natural scenario).

In terms of soil conservation, the spatial pattern changed significantly under the three scenarios. The range of soil conservation in the conservation scenario was 0 t to  $8.989 \times 10^7$  t. The range decreased significantly, but the density of the high-value distribution area increased. The range of soil conservation in the development scenario, which was 0 t to 318,954 t, was partially reduced in the distribution area of its high values compared with the situation in 2015. Soil conservation under the natural scenario ranged from 0 t to  $9.147 \times 10^6$  t; the high values were mainly concentrated in the western and northern parts of the study area, and the low values were mainly distributed in the southeastern plains of the study area. Soil conservation showed a certain trend of increase under the conservation

scenario, indicating that the soil conservation capacity of the study area could be improved by relevant ecological policy constraints (Figure 4).

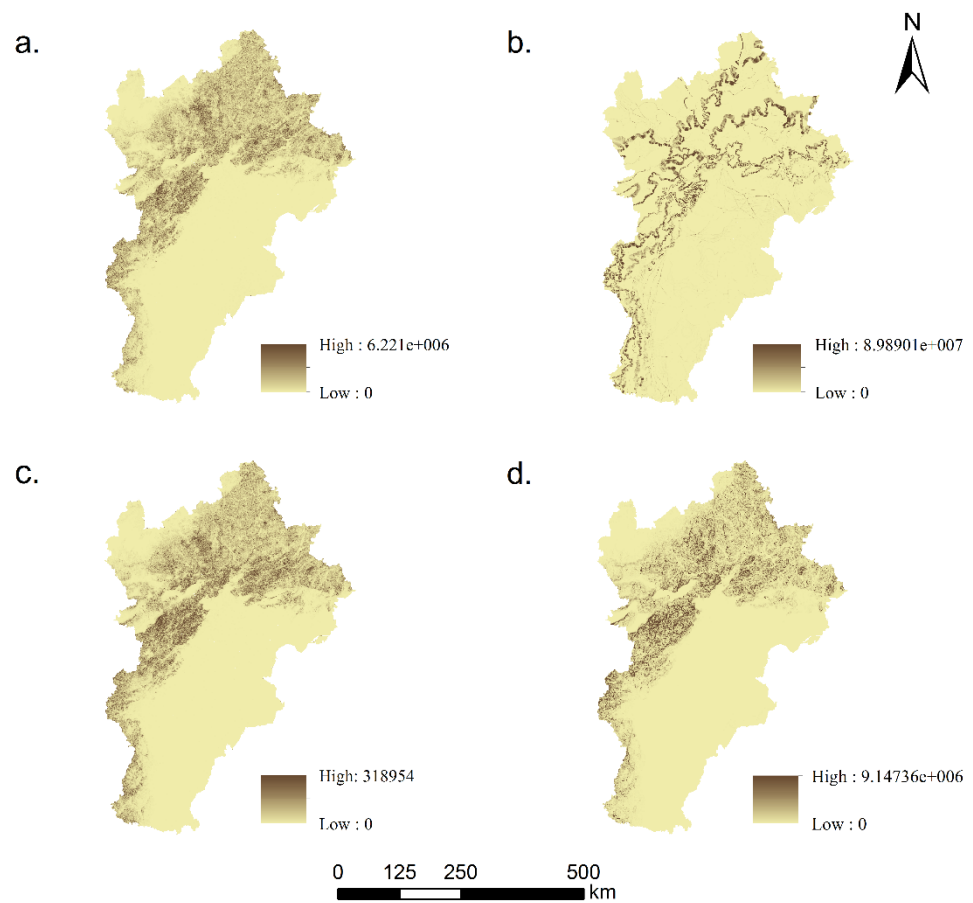


**Figure 4.** Distribution of soil conservation under different scenarios. (a) 2015; (b) conservation scenario; (c) development scenario; (d) natural scenario.

The distribution of carbon storage under different scenarios is shown in Figure 5. The carbon storage under the conservation scenario gradually shifted its high-value area from the central area to the western area compared with 2015. In addition, the lowest value was higher than the highest value in 2015. The carbon storage distribution changed considerably under the development scenario, and the high value areas greatly decreased (34,204 Mg to 198,100 Mg). Carbon storage in the natural scenario did not change much compared with 2015.

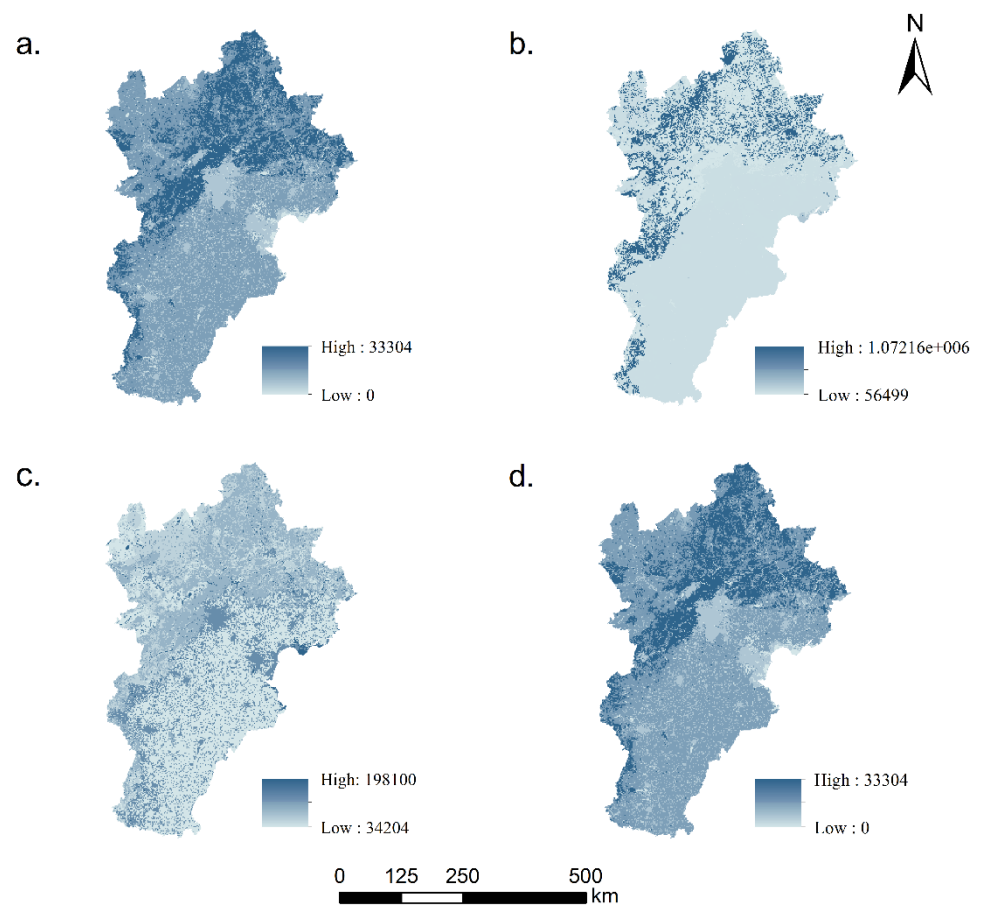


**Figure 5.** Distribution of carbon storage under different scenarios. (a) 2015; (b) conservation scenario; (c) development scenario; (d) natural scenario.

### 3.3. Ecosystem Service Trade-Off Relationships

Non-parametric tests were performed on the ecosystem service capacities of water yield, carbon storage, and soil conservation. The tests revealed that all three data series did not follow the normal distribution. Therefore, the Pearson correlation analysis tool in R was used to determine whether a trade-off occurred among the various ecosystem services. The results are shown in Figures 6 and 7.

The results revealed a high correlation among all services. The correlation coefficient ( $R > 0$ ) for each ecosystem service under the conservation scenario indicated a synergistic relationship among ecosystem services. Under the development scenario, the correlation coefficient between water yield and carbon storage was  $R = -0.61$ , and the correlation coefficient between water yield and soil conservation was  $R = -0.17$ , indicating a certain trade-off between water yield and these two services. By contrast, the correlation coefficients between water yield and carbon storage and between water yield and soil retention in the natural scenario were negative and had values of  $-0.19$  and  $-0.086$ , respectively. These results suggest that the relationships among ecosystem services shifted in the conservation scenario.

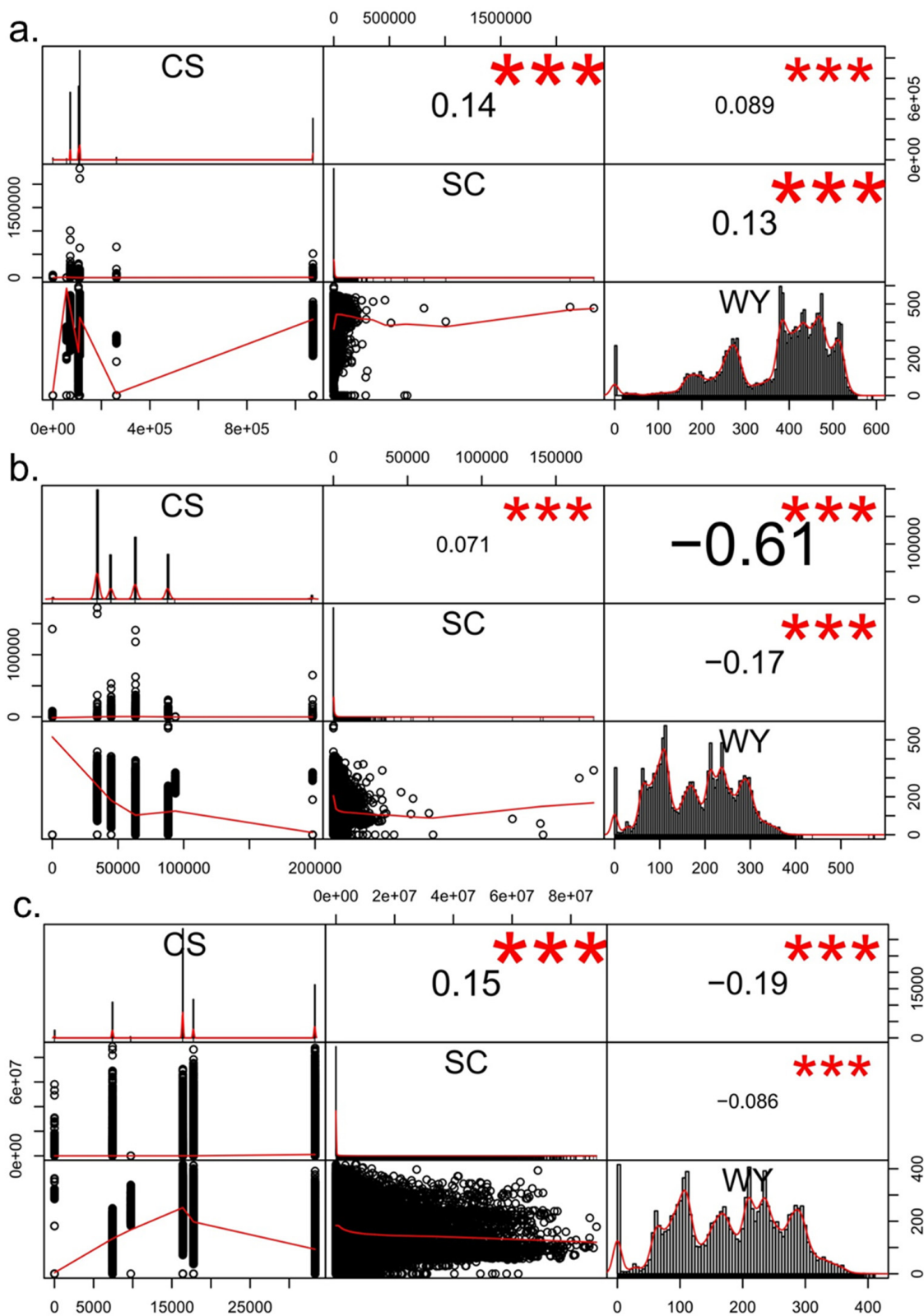


**Figure 6.** Relationship between the three ecosystem services in different scenarios. The number of \* in the figure is significant level of correlation. CS: carbon storage; SC: soil conservation; WY: water yield. (a) conservation scenario; (b) development scenario; (c) natural scenario.

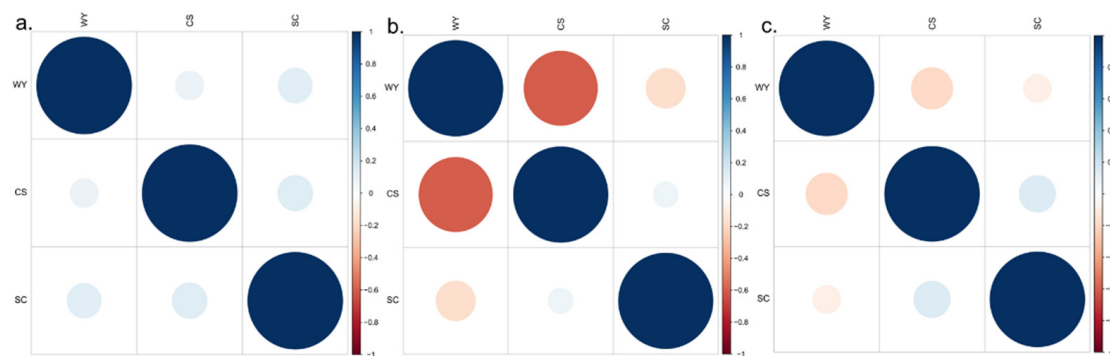


**Figure 7.** Correlation heat map between the three ecosystem services in different scenarios. CS: carbon storage; SC: soil conservation; WY: water yield. Blue indicates a positive correlation, and red indicates a negative correlation. (a) conservation scenario; (b) development scenario; (c) natural scenario.

### 3.4. Ecosystem Service Trade-Off Strength and Optimal Allocation

The results of the correlation between ecosystem services showed trade-offs between water yield and carbon storage and between water yield and soil storage in the natural and development scenarios. The optimal configuration curve between the two ecosystem services was plotted to illustrate the optimal configuration of ecosystem services. In the PPF curve, the maximum productivity of service supply was represented by the points on the curve. The situation where the service could be provided but not at the optimal allocation at this point was indicated by the points inside the curve. The situation where the service could not be provided with limited land resource allocation was indicated by the points outside the curve.

The results showed trade-offs between carbon storage and water yield services and between soil conservation and water yield services only in the natural and development scenarios. Therefore, trade-off curves were drawn according to the normalization of ecosystem services. The trade-off curves among the different ecosystem services in the two scenarios were different. The PPF curves between carbon storage and water yield for the natural and development scenarios are shown in Figure 8. The slope of the curve for the natural scenario decreased, indicating that the trade-off was gradually decreasing. Meanwhile, the slope of the curve increased gradually under the development scenario, indicating that the trade-off was gradually increasing. The PPF curves between soil conservation and water yield for the two scenarios are shown in Figure 9. The lower part of the curve in the development scenario is concave. By contrast, the upper part of the curve in the natural scenario is concave, showing that the trade-off relationship between the two services is gradually becoming significant. The mean points in the development and natural scenarios represented by points A and B, respectively, are located below the corresponding curves. In both cases, the relations between carbon storage and water yield and between soil retention and water yield do not reach the PPF curve. This scenario shows that the two services are not in an optimal configuration, indicating the potential for optimization. In Figure 8, under the development scenario, the cumulative water yield at point A1 is similar to that at point A, and the cumulative carbon storage at point A2 is similar to that at point A. The trade-off relationship between water yield and carbon storage under the development scenario is the best at points A1 and A2. Similarly, the trade-offs between water yield and carbon storage under the natural scenario are optimally configured at points B1 and B2. In Figure 9, under the development scenario, the cumulative water yield of point A1 is similar to that of point A. In addition, the cumulative soil conservation of point A2 is similar to that of point A. Points A1 and A2 are the best trade-off relationships between water yield and soil conservation under the development scenario. Similarly, points B1 and B2 are the optimal allocation points for the trade-off relationship between water yield and soil conservation under natural scenarios.

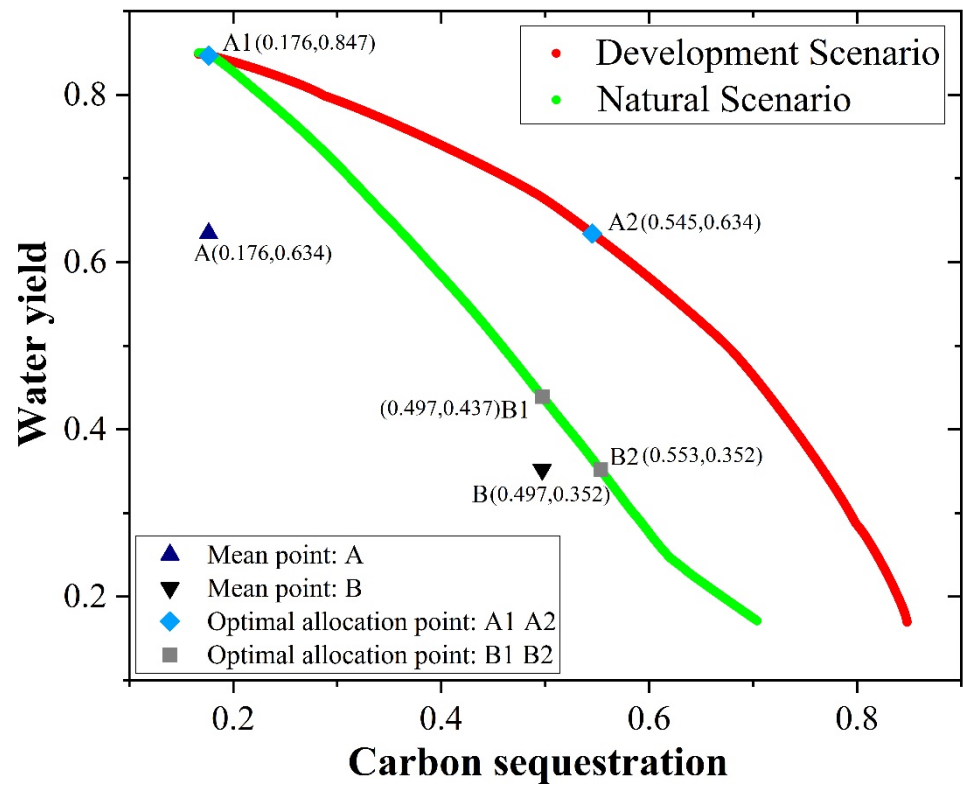


Figure 8. Trade-off curve between water yield and carbon storage under different scenarios.

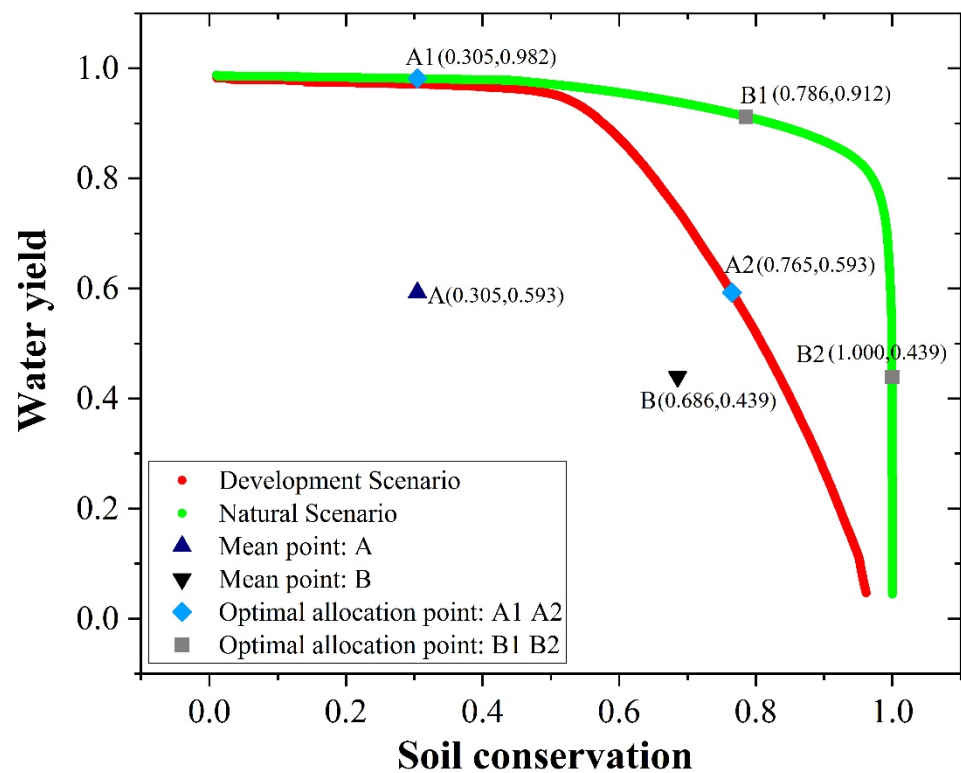


Figure 9. Trade-off curve between soil conservation and water yield under different scenarios.

Table 6 presents the intensity of the trade-off between carbon storage and water yield, that is, natural scenario (0.051) < development scenario (0.199). The strength of the trade-off between soil conservation and water yield follows the order natural scenario

(0.214) < development scenario (0.423), indicating that the mean point under the natural scenario is close to the PPF curve.

**Table 6.** Strength of the trade-off between ecosystem services under different scenarios.

Trade-Off	Trade-off Intensity Index		
	Development Scenario	Conservation Scenario	Natural Scenario
Carbon storage and water yield	0.199	/	0.051
Soil conservation and water	0.423	/	0.214

#### 4. Discussion

Nowadays, the method of combining land-use scenario simulation and ecosystem service assessment is becoming widely used [52–54]. The future relationship between land-use and ecosystem services can be explored by this method [55]. In this study, land-use data in 2005 and 2015 were selected to analyze the 10-year land-use changes in the Beijing–Tianjin–Hebei region, and the land-use transfer matrix was derived. The CLUMondo model was adopted to simulate the land-use map under different scenarios in 2035 in accordance with the transfer matrix. The CLUMondo model’s setting for land demand avoided the limitation of the land-use area. At the same time, it combined land-use change with multiple land-use demands so that spatial and temporal land-use changes in multiple scenarios could be simulated accurately [56]. Under the conservation scenario, the expansion of built-up land was restrained to a certain extent, and the proportion of forest land increased. The highest amount of carbon storage services was found in this scenario, and the high-value areas were mainly distributed in forest land, indicating that the supply benefits of carbon storage services could be enhanced by woodland. This outcome is consistent with the results of Deng et al. [57]. The highest values of water yield were found in the development scenario, and most of the high-value areas were located on woodland, which is consistent with the research results of Gao et al. [58]. Water yield can be affected by evapotranspiration from the surface, soil root depth, and soil porosity [59]. In addition, the soil porosity of built-up land is small [60]. Since built-up areas are usually regarded as areas with zero water retention capacity, where artificial building growth leads to an increase in the impervious surface, which reduces the amount of precipitation evaporation, and infiltration, leading to an increase in water yield.

The dominant functions in each region in the development process of the Beijing–Tianjin–Hebei region can be determined through the division of ecological function zones. The blind expansion of urban built-up land must be managed and controlled, and the protection of arable land and natural habitat should be strengthened to reduce the loss of ecosystem services. Then, the overall arrangement and deployment of the land-use structure layout can be implemented to avoid planning beyond the maximum range that the ecosystem services can tolerate. The integrity of the ecosystem structure and the continuity of the process can be improved and maintained by planning urban land-use, adhering to ecological priorities, promoting the development of economical and intensive land-use, and effectively enhancing ecosystem service functions.

The synergy and trade-off among various ecosystem services can be studied quantitatively by introducing PPF. Apart from macro analyses, such as correlation, the degree of influence among various ecosystem services was analyzed [61]. PPF can be combined with other model frameworks or decision-making systems to determine the optimal combination of ecosystem services and ultimately provide a scientific basis for improving the environment and ecological restoration. In most previous studies, production possibility boundaries were used primarily to evaluate the trade-offs or synergies between ecosystem services qualitatively [62]. In essence, they only compare the benefits of different programs or goals, weigh the advantages and disadvantages of various service combinations, and identify the best solution. However, the strength of the balance has not been determined

yet. In the future, the strength of the trade-off at each point can be determined through PPF, and the nature of the trade-off can be expressed visually [20]. The coefficients of the objective function for the new optimization simulation can be adjusted according to preference information, and the operation can be repeated to obtain the most ideal solution [63]. A wide range of land-use policies can be evaluated through PPF, which can accurately extract key factors in ecological, agronomic, and economic coupling systems. Its application closely links multiple fields, thus allowing scholars to conduct interdisciplinary research and analysis. In addition, the use of PPF can prevent the complicated conceptualization of problems.

Most models have certain limitations due to many factors. First, the research and development of the InVEST model entail a certain geographical orientation, and a certain degree of inapplicability emerges when evaluating the characteristics of ecosystem services in different regions. Second, to reduce the difficulty of using the model, developers simplified the calculation process of the various ecological services of the simulated ecosystem, leading to the lack of scientific calculation results. Lastly, the carbon sequestration module does not fully consider the dynamic changes in the carbon sequestration rate of different vegetation types and the impact of the carbon cycle process between different carbon pools, resulting in uncertainty in the final assessment results [64]. The shortcoming of this work is that the number of research scenarios was insufficient. Moreover, the conversion resistance parameter was set in accordance with the results of the land-use transfer matrix of the study area in 2005–2015. To make the model run successfully and achieve the expected results, the parameters were debugged several times until the final results were obtained. In this process, several human factors that could interfere with the simulation results were added, which also exerted some influence. In future research, a larger number of scenarios will be set, additional ecosystem service trade-offs will be considered for expansion, and scientific and authoritative methods will be explored further to convert resistance parameter values and make the final results more convincing.

## 5. Conclusions

Three ecosystem services, namely, water yield, soil conservation, and carbon storage, in 2015 were estimated for the Beijing–Tianjin–Hebei region. The estimation was used to simulate the three ecosystem services under three different scenarios (conservation, development, and natural scenarios) in 2035 and determine the relationship between two ecosystem services. The trade-offs were expressed visually through PPF, which also revealed changes in the ecosystem services under different land-use patterns. This research simulated the analysis of the trade-off intensity of ecosystem service value under three land-use scenarios and can be extended to explore the trade-off relationship between ecosystem services under additional scenarios in the future. The main conclusions are as follows.

- (1) Under the development scenario in 2035, the sprawl of urbanized land in the Beijing–Tianjin–Hebei region will accelerate. This expansion will lead to the occupation of a large amount of arable land and woodland, which is not conducive to the construction of ecological civilization and the sustainable and healthy development of cities in the future. Hence, experts need to plan and control the conversion of a certain amount of arable land and woodland into built-up land.
- (2) A trade-off relationship exists between water yield and soil conservation and between water yield and carbon storage services under development and natural scenarios. Synergistic relationships exist among ecosystem services under the conservation scenario. In addition, the trade-off and synergy relationships can be transformed under different land-use scenarios.
- (3) In this study, the conservation scenario was found to have the highest value of carbon storage and soil conservation, and the water yield was also at a high level. Woodland is an important supply area for carbon storage. It has high soil and water conservation capacity. Hence, appropriate measures should be implemented to improve the soil



and water conservation function in the region while enhancing the value of ecosystem services by returning the land to the forest to a certain extent.

- (4) The PPF curves between ecosystem services under different scenarios in 2035 were plotted, and the trade-off intensity of ecosystem services was calculated. In particular, visual representation of the results of agricultural planning decisions through PPF can help guide the direction of subsequent interdisciplinary research and policy. The findings showed that by controlling the conversion of land-use types, the planning goals of ecological service functions can be achieved. This work provides an important theoretical basis for the sustainable development of land resources in the Beijing–Tianjin–Hebei region.

**Author Contributions:** Conceptualization, J.W. and Z.F.; methodology, J.W., X.J. and Z.F.; software, X.J., T.C., C.W., D.F. and J.L.; formal analysis, J.W.; data curation, J.W. and C.W.; writing—original draft, J.W.; writing—review and editing, X.J. and Z.F.; visualization, J.W. and D.F.; funding acquisition, Z.F. All authors have read and agreed to the published version of the manuscript.

**Funding:** This research was funded by the Beijing Social Science Fund Project, grant number 19GLC056, the National Natural Science Foundation of China, grant number 41901261 and 42071284, the Fundamental Research Funds for the Central Universities of China, grant number 35832020024 and a grant from Beijing Key Laboratory of Spatial Development for Capital Region, grant number CLAB202010 and The APC was funded by Zhe Feng.

**Data Availability Statement:** Not applicable.

**Conflicts of Interest:** The authors declare no conflict of interest.

## References

- Bennett, E.M.; Peterson, G.D.; Gordon, L.J. Understanding relationships among multiple ecosystem services. *Ecol. Lett.* **2009**, *12*, 1394–1404. [[CrossRef](#)] [[PubMed](#)]
- Mononen, L.; Auvinen, A.P.; Ahokumpu, A.L.; Ronka, M.; Aarras, N.; Tolvanen, H.; Kamppinen, M.; Viirret, E.; Kumpula, T.; Vihervaara, P. National ecosystem service indicators: Measures of social–ecological sustainability. *Ecol. Indic.* **2014**, *61*, 27–37. [[CrossRef](#)]
- Costanza, R.; D’Arge, R.; Groot, R.D.; Farber, S.; Grasso, M.; Hannon, B.; Limburg, K.; Naeem, S.; O’Neill, R.V.; Paruelo, J.; et al. The value of the world’s ecosystem services and natural capital. *Ecol. Econ.* **1997**, *25*, 3–15. [[CrossRef](#)]
- Galic, N.; Salice, C.J.; Birnir, B.; Bruins, R.J.F.; Ducrot, V.; Jager, H.I.; Kanarek, A.; Pastorok, R.; Rebarber, R.; Thorbek, P.; et al. Predicting impacts of chemicals from organisms to ecosystem service delivery: A case study of insecticide impacts on a freshwater lake. *Sci. Total Environ.* **2019**, *682*, 426–436. [[CrossRef](#)]
- Corvalan, C.; Hales, S.; McMichael, A.J.; Butler, C.; McMichael, A. *Ecosystems and Human Well-Being: Health Synthesis*; World Health Organization: Geneva, Switzerland, 2005; Volume 34, p. 534.
- Haines-Young, R.; Potschin-Young, M.B. Revision of the Common International Classification for Ecosystem Services (CICES V5.1): A Policy Brief. *One Ecosyst.* **2018**, *3*, e27108. [[CrossRef](#)]
- Kaval, P. Integrated catchment management and ecosystem services: A twenty-five year overview. *Ecosyst. Serv.* **2019**, *37*. [[CrossRef](#)]
- Fisher, B.; Turner, R.K.; Morling, P. Defining and classifying ecosystem services for decision making. *Ecol. Econ.* **2009**, *68*, 643–653. [[CrossRef](#)]
- Ouyang, Z.; Zheng, H.; Xiao, Y.; Polasky, S.; Liu, J.; Xu, W.; Wang, Q.; Zhang, L.; Xiao, Y.; Rao, E.; et al. Improvements in ecosystem services from investments in natural capital. *Science* **2016**, *352*, 1455–1459. [[CrossRef](#)] [[PubMed](#)]
- Li, S.; Li, X.; Dou, H.; Dang, D.; Gong, J. Integrating constraint effects among ecosystem services and drivers on seasonal scales into management practices. *Ecol. Indic.* **2021**, *125*, 107425. [[CrossRef](#)]
- Hao, R.; Yu, D.; Liu, Y.; Yang, L.; Qiao, J.; Wang, X.; Du, J. Impacts of changes in climate and landscape pattern on ecosystem services. *Sci. Total Environ.* **2017**, *579*, 718–728. [[CrossRef](#)]
- Cao, Y.; Cao, Y.; Li, G.; Tian, Y.; Fang, X.; Li, Y.; Tan, Y. Linking ecosystem services trade-offs, bundles and hotspot identification with cropland management in the coastal Hangzhou Bay area of China. *Land Use Policy* **2020**, *97*, 104689. [[CrossRef](#)]
- Xu, S.; Liu, Y.; Wang, X.; Zhang, G. Scale effect on spatial patterns of ecosystem services and associations among them in semi-arid area: A case study in Ningxia Hui Autonomous Region, China. *Sci. Total Environ.* **2017**, *598*, 297–306. [[CrossRef](#)] [[PubMed](#)]
- Shen, j.; Li, S.; Liu, L.; Liang, Z.; Wang, Y.; Wang, H.; Wu, S. Uncovering the relationships between ecosystem services and social-ecological drivers at different spatial scales in the Beijing-Tianjin-Hebei region. *J. Clean. Prod.* **2020**, *290*, 125193. [[CrossRef](#)]
- Loomes, R.; O’Neill, K. Nature’s Services: Societal Dependence on Natural Ecosystems. *Pac. Conserv. Biol.* **1997**, *6*, 220–221. [[CrossRef](#)]

16. Haines-Young, R.; Potschin, M.; Kienast, F. Indicators of ecosystem service potential at European scales: Mapping marginal changes and trade-offs. *Ecol. Indic.* **2012**, *21*, 39–53. [[CrossRef](#)]
17. Willemsen, L.; Hein, L.; Mensvoort, M.E.F.; Verburg, P.H. Space for people, plants, and livestock? Quantifying interactions among multiple landscape functions in a Dutch rural region. *Ecol. Indic.* **2010**, *10*, 62–73. [[CrossRef](#)]
18. Tallis, H.; Kareiva, P.; Marvier, M.; Chang, A. Ecosystem Services Special Feature: An ecosystem services framework to support both practical conservation and economic development. *Proc. Natl. Acad. Sci. USA* **2008**, *105*, 9457–9464. [[CrossRef](#)] [[PubMed](#)]
19. Howe, C.; Suich, H.; Vira, B.; Mace, G.M. Creating win-wins from trade-offs? Ecosystem services for human well-being: A meta-analysis of ecosystem service trade-offs and synergies in the real world. *Glob. Environ. Chang.* **2014**, *28*, 263–275. [[CrossRef](#)]
20. Yang, W.; Jin, Y.; Sun, T.; Yang, Z.; Cai, Y.; Yi, Y. Trade-offs among ecosystem services in coastal wetlands under the effects of reclamation activities. *Ecol. Indic.* **2018**, *92*, 354–366. [[CrossRef](#)]
21. Zhong, L.; Wang, J.; Zhang, X.; Ying, L. Effects of agricultural land consolidation on ecosystem services: Trade-offs and synergies. *J. Clean. Prod.* **2020**, *264*, 121412. [[CrossRef](#)]
22. Li, B.; Chen, N.; Wang, Y.; Wang, W. Spatio-temporal quantification of the trade-offs and synergies among ecosystem services based on grid-cells: A case study of Guanzhong Basin, NW China. *Ecol. Indic.* **2018**, *94*, 246–253. [[CrossRef](#)]
23. Zavalloni, M.; Groeneveld, R.A.; Zwieten, P.V. The role of spatial information in the preservation of the shrimp nursery function of mangroves: A spatially explicit bio-economic model for the assessment of land use trade-offs. *J. Environ. Manag.* **2014**, *143*, 17–25. [[CrossRef](#)]
24. Marshall, A. *Principles of Economics*, 8th ed.; McMillan: London, UK, 2013.
25. Zhou, Z.X.; Li, J.; Guo, Z.Z.; Li, T. Trade-offs between carbon, water, soil and food in Guanzhong-Tianshui economic region from remotely sensed data. *Int. J. Appl. Earth Obs. Geoinf.* **2017**, *58*, 145–156. [[CrossRef](#)]
26. Basse, R.M.; Omrani, H.; Charif, O.; Gerber, P.; Bódis, K. Land use changes modelling using advanced methods: Cellular automata and artificial neural networks. The spatial and explicit representation of land cover dynamics at the cross-border region scale. *Appl. Geogr.* **2014**, *53*, 160–171. [[CrossRef](#)]
27. Cavender-Bares, J.; Polasky, S.; King, E.; Balvanera, P. A sustainability framework for assessing trade-offs in ecosystem services. *Ecol. Soc.* **2015**, *20*. [[CrossRef](#)]
28. Stosch, K.C.; Quilliam, R.S.; Bunnefeld, N.; Oliver, D.M. Quantifying stakeholder understanding of an ecosystem service trade-off. *Sci. Total Environ.* **2018**, *651*, 2524–2534. [[CrossRef](#)]
29. Zeng, L.; Li, J.; Zhou, Z.; Yu, Y. Optimizing land use patterns for the grain for Green Project based on the efficiency of ecosystem services under different objectives. *Ecol. Indic.* **2020**, *114*, 106347. [[CrossRef](#)]
30. Peng, J.; Hu, X.; Wang, X.; Meersmans, J.; Liu, Y.; Qiu, S. Simulating the impact of Grain-for-Green Programme on ecosystem services trade-offs in Northwestern Yunnan, China. *Ecosyst. Serv.* **2019**, *39*, 100998. [[CrossRef](#)]
31. Clerici, N.; Cote-Navarro, F.; Escobedo, F.J.; Rubiano, K.; Villegas, J.C. Spatio-temporal and cumulative effects of land use-land cover and climate change on two ecosystem services in the Colombian Andes. *Sci. Total Environ.* **2019**, *685*, 1181–1192. [[CrossRef](#)] [[PubMed](#)]
32. Pham, H.V.; Sperotto, A.; Torresan, S.; Acua, V.; Jorda-Capdevila, D.; Rianna, G.; Marcomini, A.; Critto, A. Coupling scenarios of climate and land-use change with assessments of potential ecosystem services at the river basin scale. *Ecosyst. Serv.* **2019**, *40*, 101045. [[CrossRef](#)]
33. Liu, H.; Zheng, L.; Wu, J.; Liao, Y. Past and future ecosystem service trade-offs in Poyang Lake Basin under different land use policy scenarios. *Arab. J. Geosci.* **2020**, *13*, 46. [[CrossRef](#)]
34. Haase, D.; Schwarz, N.; Strohbach, M.; Kroll, F.; Seppelt, R. Synergies, Trade-offs, and Losses of Ecosystem Services in Urban Regions: An Integrated Multiscale Framework Applied to the Leipzig-Halle Region, Germany. *Ecol. Soc.* **2012**, *17*. [[CrossRef](#)]
35. Morán-Ordóez, A.; Ameztegui, A.; Cáceres, M.; De-Miguel, S.; Lefèvre, F.; Brotons, L.; Coll, L. Future trade-offs and synergies among ecosystem services in Mediterranean forests under global change scenarios. *Ecosyst. Serv.* **2020**, *45*, 101174. [[CrossRef](#)]
36. Pickard, B.R.; Berkel, D.V.; Petrasova, A.; Meentemeyer, R.K. Forecasts of urbanization scenarios reveal trade-offs between landscape change and ecosystem services. *Landsc. Ecol.* **2017**, *32*, 617–634. [[CrossRef](#)]
37. Vliet, J.V.; Verburg, P.H. A Short Presentation of CLUMondo. *Geomat. Approaches Model. Land Chang. Scenar.* **2018**, 485–492. [[CrossRef](#)]
38. Van Asselen, S.; Verburg, P.H. Land cover change or land-use intensification: Simulating land system change with a global-scale land change model. *Glob. Chang. Biol.* **2013**, *19*, 3648–3667. [[CrossRef](#)]
39. Wang, C.; Yu, C.; Chen, T.; Feng, Z.; Wu, K. Can the establishment of ecological security patterns improve ecological protection? An example of Nanchang, China. *Sci. Total Environ.* **2020**, *740*, 140051. [[CrossRef](#)]
40. Domingo, D.; Palka, G.; Hersperger, A.M. Effect of zoning plans on urban land-use change: A multi-scenario simulation for supporting sustainable urban growth. *Sustain. Cities Soc.* **2021**, *69*, 102833. [[CrossRef](#)]
41. Malek, Ž.; Verburg, P.H.; Geijzendorffer, I.R.; Bondeau, A.; Cramer, W. Global change effects on land management in the Mediterranean region. *Glob. Environ. Chang.* **2018**, *50*, 238–254. [[CrossRef](#)]
42. Jin, X.; Li, X.; Feng, Z.; Wu, J.; Wu, K. Linking ecological efficiency and the economic agglomeration of China based on the ecological footprint and nighttime light data. *Ecol. Indic.* **2020**, *111*, 106035. [[CrossRef](#)]
43. Feng, Z.; Jin, X.; Chen, T.; Wu, J. Understanding trade-offs and synergies of ecosystem services to support the decision-making in the Beijing–Tianjin–Hebei region. *Land Use Policy* **2021**, *106*, 105446. [[CrossRef](#)]

44. Guan, D.; Gao, W.; Kazuyuki, W.; Hidetoshi, F. Land use change of Kitakyushu based on landscape ecology and Markov model. *J. Geogr. Sci.* **2008**, *18*, 455–468. [[CrossRef](#)]
45. Chen, K. *Simulation of Land Use Change in Coastal Area of Guangxi Beibu Gulf Based on CLUMondo Model*; Guangxi University: Nanning, China, 2018.
46. Haiming, Y.; Jinyan, Z.; Qun'ou, J. International Society for Environmental Information Sciences 2010 Annual Conference (ISEIS) Scenario simulation of change of forest land in Poyang Lake watershed. *Procedia Environ. Sci.* **2010**, *2*, 1469–1478. [[CrossRef](#)]
47. Chen, T.; Feng, Z.; Zhao, H.; Wu, K. Identification of ecosystem service bundles and driving factors in Beijing and its surrounding areas. *Sci. Total Environ.* **2020**, *711*, 134687. [[CrossRef](#)]
48. Sharp, R.; Chaplin-Kramer, R.; Wood, S.; Guerry, A.; Douglass, J. *InVEST User's Guide*; 2018; Available online: [https://invest-userguide.readthedocs.io/\\_/downloads/en/3.5.0/pdf/](https://invest-userguide.readthedocs.io/_/downloads/en/3.5.0/pdf/) (accessed on 21 August 2021).
49. Williams, J.R.; Arnold, J.G. A system of erosion—sediment yield models. *Soil Technol.* **1997**, *11*, 43–55. [[CrossRef](#)]
50. Wang, C.; Zhan, J.; Chu, X.; Liu, W.; Zhang, F. Variation in ecosystem services with rapid urbanization: A study of carbon sequestration in the Beijing–Tianjin–Hebei region, China. *Phys. Chem. Earth Parts A/B/C* **2019**, *110*, 195–202. [[CrossRef](#)]
51. Yang, W.; Jin, Y.; Sun, L.; Sun, T.; Shao, D. Determining the intensity of the trade-offs among ecosystem services based on production-possibility frontiers: Model development and a case study. *J. Nat. Resour.* **2019**, *034*, 2516–2528. [[CrossRef](#)]
52. Nijhum, F.; Westbrook, C.; Noble, B.; Belcher, K.; Lloyd-Smith, P. Evaluation of alternative land-use scenarios using an ecosystem services-based strategic environmental assessment approach. *Land Use Policy* **2021**, *108*, 105540. [[CrossRef](#)]
53. Newbold, T.; Hudson, L.N.; Hill, S.L.L.; Contu, S.; Lysenko, I.; Senior, R.A.; Börger, L.; Bennett, D.J.; Choimes, A.; Collen, B.; et al. Global effects of land use on local terrestrial biodiversity. *Nature* **2015**, *520*, 45–50. [[CrossRef](#)]
54. Wang, Y.; Li, X.; Zhang, Q.; Li, J.; Zhou, X. Projections of future land use changes: Multiple scenarios-based impacts analysis on ecosystem services for Wuhan city, China. *Ecol. Indic.* **2018**, *94*, 430–445. [[CrossRef](#)]
55. Esmail, B.A.; Geneletti, D. Design and impact assessment of watershed investments: An approach based on ecosystem services and boundary work. *Environ. Impact Assess. Rev.* **2017**, *62*, 1–13. [[CrossRef](#)]
56. Zhu, W.; Gao, Y.; Zhang, H.; Liu, L. Optimization of the land use pattern in Horqin Sandy Land by using the CLUMondo model and Bayesian belief network. *Sci. Total Environ.* **2020**, *739*, 139929. [[CrossRef](#)] [[PubMed](#)]
57. Deng, Y.; Yao, S.; Hou, M.; Zhang, T.; Lu, Y.; Gong, Z.; Wang, Y. Assessing the effects of the Green for Grain Program on ecosystem carbon storage service by linking the InVEST and FLUS models: A case study of Zichang county in hilly and gully region of Loess Plateau. *J. Nat. Resour.* **2020**, *35*, 75–93. [[CrossRef](#)]
58. Gao, J.; Li, F.; Gao, H.; Zhou, C.; Zhang, X. The impact of land-use change on water-related ecosystem services: A study of the Guishui River Basin, Beijing, China. *J. Clean. Prod.* **2016**, *163*, S148–S155. [[CrossRef](#)]
59. Taye, G.; Poesen, J.; Wesemael, B.V.; Vanmaercke, M.; Tekla, D.; Deckers, J.; Goosse, T.; Maetens, W.; Nyssen, J.; Hallet, V.; et al. Effects of land use, slope gradient, and soil and water conservation structures on runoff and soil loss in semi-arid Northern Ethiopia. *Phys. Geogr.* **2013**, *34*, 236–259. [[CrossRef](#)]
60. Wang, B.; Chen, H.; Dong, Z.; Zhu, W.; Qiu, Q.; Tang, L. Impact of land use change on the water conservation service of ecosystems in the urban agglomeration of the Golden Triangle of Southern Fujian, China, in 2030. *Acta Ecol. Sin.* **2020**, *40*, 484–498. [[CrossRef](#)]
61. Vallet, A.; Locatelli, B.; Levrel, H.; Wunder, S.; Seppelt, R.; Scholes, R.J.; Oszwald, J. Relationships Between Ecosystem Services: Comparing Methods for Assessing Tradeoffs and Synergies. *Ecol. Econ.* **2018**, *150*, 96–106. [[CrossRef](#)]
62. King, E.; Cavender-Bares, J.; Balvanera, P.; Mwampamba, T.H.; Polasky, S. Trade-offs in ecosystem services and varying stakeholder preferences: Evaluating conflicts, obstacles, and opportunities. *Ecol. Soc.* **2015**, *20*. [[CrossRef](#)]
63. Nguyen, T.H.; Cook, M.; Field, J.L.; Khuc, Q.V.; Paustian, K. High-resolution trade-off analysis and optimization of ecosystem services and disservices in agricultural landscapes. *Environ. Model. Softw.* **2018**, *107*, 105–118. [[CrossRef](#)]
64. Sharps, K.; Masante, D.; Thomas, A.R.C.; Jackson, B.M.; Cosby, B.J.; Emmett, B.A.; Jones, L. Comparing strengths and weaknesses of three ecosystem services modelling tools in a diverse UK river catchment. *Sci. Total Environ.* **2017**, *584–585*, 118–130. [[CrossRef](#)] [[PubMed](#)]